

# Geophysical Research Letters<sup>®</sup>



## RESEARCH LETTER

10.1029/2023GL104184

### Key Points:

- Emission factors indexed by plant species are used to replace biome-scale factors to update fire emission inventory over northern Eurasia
- Updated fire emission for black carbon over northern Eurasia is 33% lower than the original inventory FEI-NE, but 61% higher than GFED
- Simulation with the new inventory shows better reproduced ground-based and satellite retrievals of aerosol absorption optical depth

### Supporting Information:

Supporting Information may be found in the online version of this article.

### Correspondence to:

X. Dong,  
dongxy@nju.edu.cn

### Citation:

Huang, R., Dong, X., Cheng, M., Li, X., Liu, Y., Wu, X., et al. (2023). A plant species dependent wildfire black carbon emission inventory in northern Eurasia. *Geophysical Research Letters*, 50, e2023GL104184. <https://doi.org/10.1029/2023GL104184>

Received 20 APR 2023

Accepted 8 SEP 2023








### Author Contributions:

**Conceptualization:** Ruqi Huang, Xinyi Dong, Manqiu Cheng  
**Data curation:** Ruqi Huang, Xinyi Dong, Manqiu Cheng  
**Formal analysis:** Ruqi Huang, Xinyi Dong, Manqiu Cheng  
**Funding acquisition:** Xinyi Dong, Minghuai Wang  
**Investigation:** Ruqi Huang, Xinyi Dong, Manqiu Cheng  
**Methodology:** Ruqi Huang, Xinyi Dong, Manqiu Cheng

© 2023. The Authors.

This is an open access article under the terms of the [Creative Commons Attribution-NonCommercial-NoDerivs License](#), which permits use and distribution in any medium, provided the original work is properly cited, the use is non-commercial and no modifications or adaptations are made.

## A Plant Species Dependent Wildfire Black Carbon Emission Inventory in Northern Eurasia

Ruqi Huang<sup>1</sup> , Xinyi Dong<sup>1,2,3</sup> , Manqiu Cheng<sup>4</sup>, Xiao Li<sup>1</sup> , Yaman Liu<sup>1</sup> , Xuexu Wu<sup>1</sup>, Yuan Liang<sup>1</sup> , Minghuai Wang<sup>1</sup> , Joshua S. Fu<sup>5,6</sup> , and Matthew Tipton<sup>5</sup>

<sup>1</sup>School of Atmospheric Sciences, Nanjing University, Nanjing, China, <sup>2</sup>Joint International Research Laboratory of Atmospheric and Earth System Sciences, Institute for Climate and Global Change Research, Nanjing University, Nanjing, China, <sup>3</sup>Frontiers Science Center for Critical Earth Material Cycling, Nanjing University, Nanjing, China, <sup>4</sup>Department of Atmospheric and Oceanic Sciences, School of Physics, Peking University, Beijing, China, <sup>5</sup>Department of Civil and Environmental Engineering, University of Tennessee, Knoxville, TN, USA, <sup>6</sup>Computational Earth Science Group, Oak Ridge National Laboratory, Oak Ridge, TN, USA

**Abstract** Wildfire emission inventories are usually applied with biome-scale emission factors for atmospheric modeling. However, emission factors measured for different plant species vary substantially within the same biome. We apply the species-specific emission factors and refine the Fire Emission Inventory-northern Eurasia (FEI-NE), and derive the wildfire black carbon emission inventory in northern Eurasia from 2002 to 2015. Our new inventory produces 61% more black carbon emissions than current estimates based on Global Fire Emission Database (GFED) and 33% less than FEI-NE. Model simulations with different inventories are compared with ground-based and satellite retrievals of aerosol absorption optical depth (AAOD). Compared with the Ozone Monitoring Instrument, the normalized root mean square deviation of AAOD over northern Eurasia is reduced from 1.0 under FEI-NE to 0.95 through application of the new inventory. This study reveals the importance of applying sub-biome-scale emission factors for wildfire inventories development and revisiting emissions uncertainty in atmospheric modeling.

**Plain Language Summary** A recent biomass burning emission inventory for black carbon in northern Eurasia was developed as FEI-NE. We found that the emission factors applied for wildfires in northern Eurasia boreal forest and grassland were adopted from the prescribed fire measurements conducted in the United States for woody savannas and wetlands, respectively. By comparing with recently published local measurements in Siberia, we mapped the emission factors for plant species from the database published by U.S. Forest Service to biomass structures in northern Eurasia and rebuilt the FEI-NE inventory as FEI-NE<sub>sp</sub>. Modeling results obtained from GEOS-Chem for 2011–2012 suggested that the simulation with FEI-NE<sub>sp</sub> agreed better with ground-based and satellite observations than FEI-NE and GFEDv4.1s.

## 1. Introduction

Black Carbon (BC) contributes significantly to the Earth's radiative budget due to its strong absorption effect (Bond et al., 2013; Huang et al., 2015; Ramanathan & Carmichael, 2008). The impacts of BC on climate are usually evaluated with atmospheric modeling, but uncertainties remain due to both emission inventory and model mechanisms. Wildfire is one of the primary sources of BC, which generates emissions through combustion processes (Bowman et al., 2009; Voulgarakis & Field, 2015). Although constraints have been implemented to reduce discrepancies between observations and emission estimates, significant uncertainties still exist in the current fire emission inventory (May et al., 2014).

In recent years, many efforts have been devoted to improving the spatial and temporal resolutions of fire emission inventories to meet the modeling needs for air quality and climate applications (van der Werf et al., 2017). Advances in satellite remote sensing have facilitated the development of updated fire emission inventories. However, there are substantial variations in BC emissions among different biomass burning inventories due to differences in remote-sensing image interpretation, adjustments made for small and obscured fires, and emission factors (EFs) which represent the amount of a compound emitted per unit dry matter consumed. EFs and biomass consumption data sets are critical inputs for models, but uncertainties arise from factors such as biofuel properties, experimental methodology, combustion facilities, and fire management behaviors (Akagi et al., 2011; Andreae & Merlet, 2001; Liu et al., 2020; Sulla-Menashe et al., 2019; van der Werf et al., 2010; Yokelson et al., 2013). A

**Project Administration:** Xinyi Dong, Minghuai Wang  
**Resources:** Ruqi Huang, Xinyi Dong, Minghuai Wang, Joshua S. Fu, Matthew Tipton  
**Software:** Ruqi Huang, Xinyi Dong, Xiao Li, Yaman Liu, Yuan Liang  
**Supervision:** Xinyi Dong, Minghuai Wang, Joshua S. Fu, Matthew Tipton  
**Validation:** Ruqi Huang, Xinyi Dong  
**Visualization:** Ruqi Huang, Xinyi Dong, Manqiu Cheng, Xuexu Wu  
**Writing – original draft:** Ruqi Huang  
**Writing – review & editing:** Ruqi Huang, Xinyi Dong, Joshua S. Fu, Matthew Tipton

lack of filed data has hindered efforts to develop accurate estimates of EFs, resulting in persistent uncertainties. Significant progress has been made in exploring the influence of combustion phases on fire emissions. Modified combustion efficiency (MCE), as an indicator of the relative fraction of flaming and smoldering combustion, has been demonstrated to correlate well with EFs (Andreae, 2019; Zheng et al., 2018, 2021). High BC emissions are often associated with flaming combustion while low BC emissions are associated with smoldering combustion (Haslett et al., 2018; Heringa et al., 2011; Li et al., 2021). In addition, the fuel types remain another essential role in the EFs uncertainty. The biome-specific EFs compiled by Akagi et al. (2011) have been widely used for emission estimation, and they were adopted by Global Fire Emissions Database (GFED) (Giglio et al., 2013). However, significant variations in plant species can occur within the same biome, and these diverse species may emit BC at different rates. It is essential to consider species-level traits when evaluating fire emissions and their impact on climate (Guenther et al., 2012; Rogers et al., 2015). To reduce uncertainty in emission inventories, it is necessary to compile lists assigning EFs to individual plant species within each biome.

United States Forest Service (USFS) recently developed the Fire Emission Inventory-northern Eurasia (FEI-NE) by using local surveying data of dominant plant species (Hao et al., 2016). However, model simulations with the FEI-NE inventory suggested that BC emissions might be overestimated in the source region due to the employment of emission factors determined from U.S. vegetation and land use data (Dong et al., 2019). As a result, there is an urgent need to improve the reliability of BC emission inventories in northern Eurasia due to its significant impact on the Arctic (Popovicheva et al., 2022). In this study, we developed a plant species-dependent biomass burning emission inventory for BC over northern Eurasia by bridging the gap between the biomass and species-specific emission factors databases. Simulations with the GEOS-Chem model were conducted using the traditional biome-dependent inventory GFED and this new inventory. Simulation results were validated against ground-based measurements and aircraft campaigns to reveal the uncertainties associated with emission factors.

## 2. Methods

### 2.1. Emission Calculations

Biomass burning emission (Emis.) for BC is usually estimated in the following form:

$$\text{Emis.} = \text{BA} \times \text{FC} \times \text{EF}$$

where EF is the emission factor, BA is the burned area, and FC is the fuel consumption.

Most global fire emission inventories used satellite products to estimate BA, such as GFED, Quick Fire Emission Data (QFED) (Darmenov & da Silva, 2015), Fire Locating and Monitoring of Burning Emissions (FLAMBE) (Reid et al., 2009), and Fire Inventory from NCAR (FINN) (Wiedinmyer et al., 2011), which primarily relied on MODIS (Moderate Resolution Imaging Spectroradiometer, available at <https://modis.gsfc.nasa.gov/data/>) products to identify fire locations and estimate temporal variations of BA. The FEI-NE inventory used MODIS thermal anomalies MOD14 and MYD14 at 1 km grid resolution with the algorithm from Urbanski et al. (2011) to map active fire and burned scars. The land cover product MOD12 was used to generate BA with land cover classification at 500 m grid resolution. Earlier versions of GFED directly adopted the MODIS burned area product MCD64A1 Collection 5 but underestimated BA due to the unintentional removal of minor burns and systematic omission errors. GFED4.1s adopted the MCD64A1 Collection 5.1 product that reduced these errors and combined it with the 1 km individual fire detections and locations product MCD14ML to statistically derive BA for small fires. In general, FEI-NE and GFED4.1s essentially developed their estimations of BA on a similar basis. Figures 1a and 1b demonstrated the spatial distributions of burned area fractions at 0.25° grid for GFED and FEI-NE, respectively, and their estimations of BA from 2002 to 2015. FEI-NE predicted a higher burned area fraction than GFED4.1s over Kazakhstan for savanna fires and over the eastern side of Lake Baikal for boreal forest fires. Annual variation agreed well between the two inventories, and BA was 22% lower on average for FEI-NE.

FC estimated by GFED4.1s and FEI-NE were shown in Figures 1d and 1e, respectively. Fuel combustion was determined by fuel loading (FL) and combustion completeness. GFED estimated FL using a modeling method based on net primary production (NPP), heterotrophic respiration (Rh), biomass burning, precipitation, temperature, solar radiation, and fractional absorbed photosynthetically active radiation. FEI-NE estimated FL through a surveying method based on MOD12 land cover product, local dominant forest species data, forest inventory

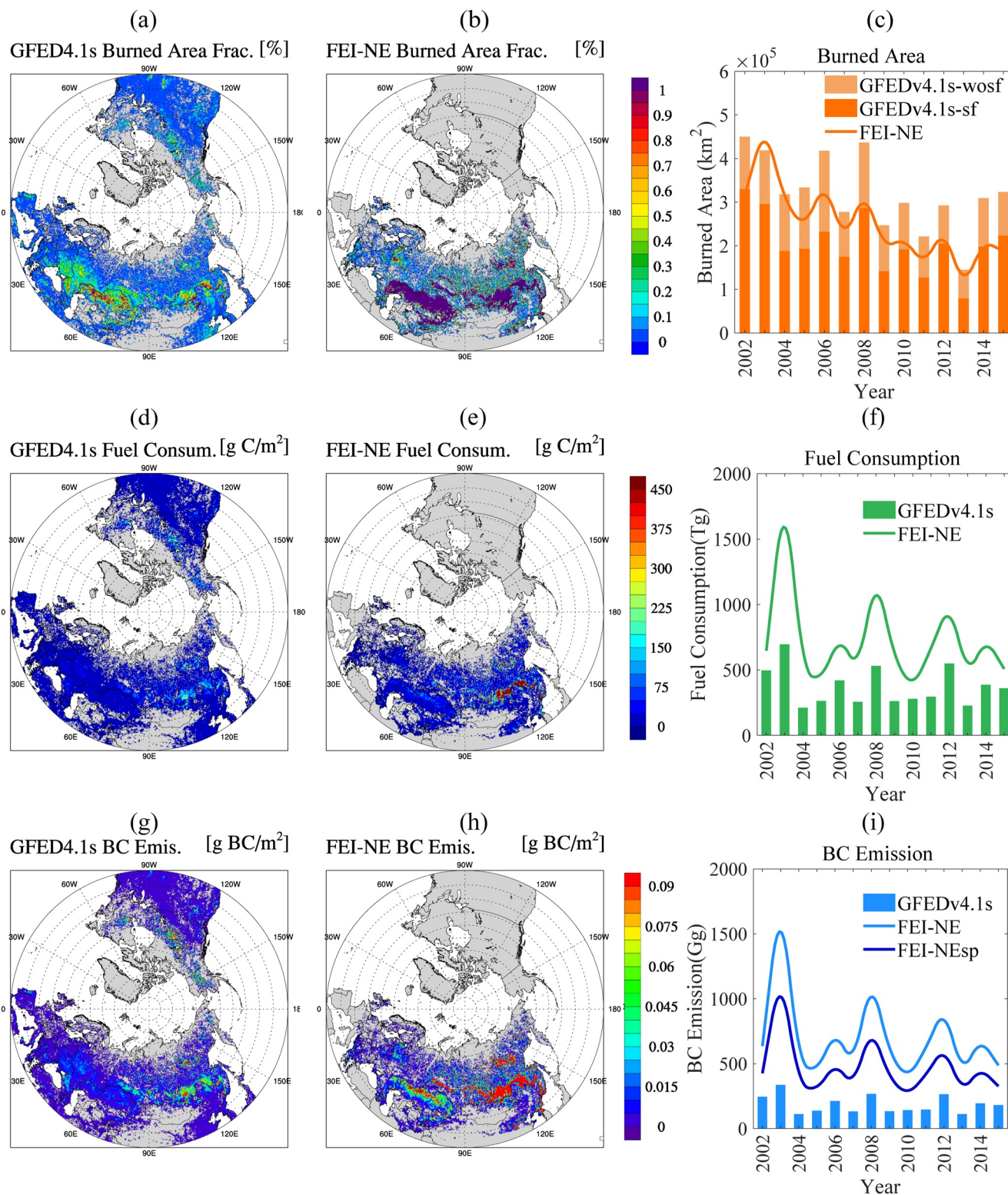


**Figure 1.** Spatial distributions of biomass burning (a, b) burned area fraction, (d, e) fuel consumption, and (g, h) BC emission averaged for 2002–2015 calculated respectively by GFEDv4.1s (left column) and FEI-NE inventory (middle column). Time series of (c) burned area, (f) fuel consumption, and (i) BC emission during 2002–2015 of the inventories in northern Eurasia. BC = Black Carbon; GFED = Global Fire Emission Database; FEI-NE = Fire Emission Inventory-northern Eurasia; FEI-NE<sub>sp</sub> = updated FEI-NE inventory based on plant species.

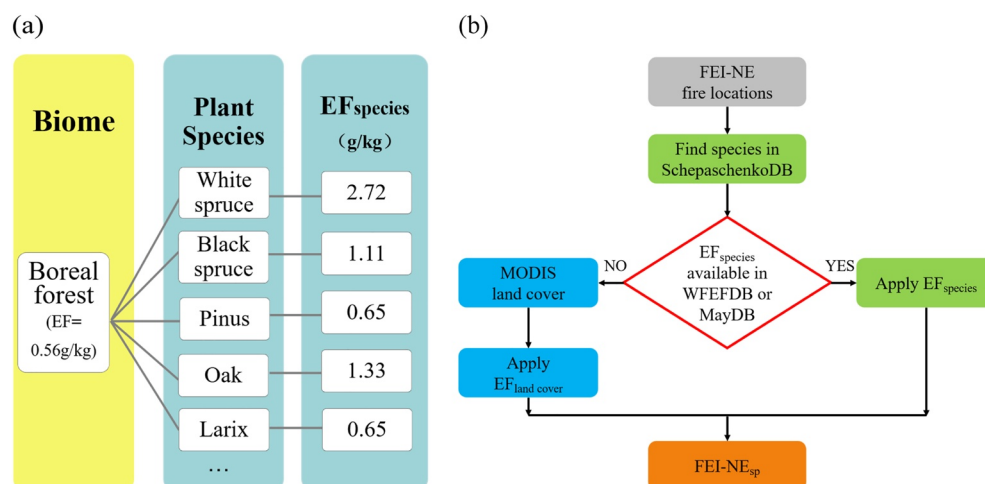


**Figure 2.** (a) Mapping relationship between the biome, plant species and emission factors. (b) Flowchart of applying species-dependent EF (EF<sub>species</sub>) and land cover-dependent EF (EF<sub>land cover</sub>) to reconstruct the FEI-NE<sub>sp</sub> for BC emission inventory.

data and the IPCC Global Biomass Carbon Map. To estimate combustion completeness, GFED applied a lookup table with upper and lower limits scaled with soil moisture for different fuel types or with MODIS vegetation scalar for boreal forest fires, while FEI-NE used the CONSUME model (Prichard et al., 2006). The estimated FC was generally consistent between GFED4.1s and FEI-NE over most of northern Eurasia, as shown in Figures 1d and 1e. However, FC used in FEI-NE was nearly twice as much as that of GFED4.1s on average over 2002–2015, indicating the significant influence by using local surveying data over northern Eurasia.

Emission factors (EFs) were typically measured in field or aircraft campaigns for prescribed and wild fires or in combustion chambers for burning experiments (Burling et al., 2010). Although most measurements recorded fuel types with dominant species information, EFs were usually compiled at the biome level for atmospheric modeling due to limited information on detailed biomass composition for wildfires. As one of the most popular EFs data sets, Akagi et al. (2011) categorized emission factors of biomass fuels into six broad types for landscape-scale fires, including tropical forest, temperate forest, boreal forest, peatlands, chaparral, and savanna. However, multiple land cover types and plant species could be found within each biome category, and different biome categories may also contain the same land cover type. For example, deciduous needle leaf forests, deciduous broad leaf forests and evergreen broad leaf forests could all be aggregated to temperate forests. Deciduous needle leaf trees (e.g., spruce, *Larix*) could also be the dominant species in some boreal forests. Consequently, EF may vary significantly among different plant species within the same biome type, leading to aggregated uncertainties. For example, as Figure 2a shows, during the same chamber measurement experiment, May et al. (2014) reported that the EF for BC was 1.11 g/kg for black spruce (*Picea mariana*) and 2.72 g/kg for white spruce (*Picea glauca*), both of which are popular tree species in North America. Nevertheless, GFED suggested that EF for boreal forest fire was 0.56 g/kg, indicating that EFs at the biome level may retain a large uncertainty.

Subsequently, while both GFED and FEI-NE used MODIS land cover data to index BA and they provided a more detailed estimation of FL, this effort was limited by the use of biome-scale EFs in the emission inventory. FEI-NE applied a coarse version of biome-level EF as 0.93 and 1.36 g/kg for forest and non-forest (savanna, shrub, and grass) fires, respectively. These EFs were derived from May et al. (2014) representing the aircraft campaign measurements collected at Bamberg (33.2°E, 80.9°W) and Georgetown (33.2°E, 79.4°W) in South Carolina, respectively, for prescribed fires in 2011. According to MODIS land cover product, the prescribed fire campaign site in Bamberg was woody savanna and the site in Georgetown was a permanent wetland. May et al. (2014) reported that the dominant fuel for the Bamberg fires was longleaf/loblolly pine understory, and for the Georgetown fire was coastal grass understory, consistent with the land cover types observed by MODIS. However, most wildfires in northern Eurasia occurred in different types of vegetation such as the boreal forests, savanna, and inland grassland. Vasileva et al. (2017) reported emission ratios (ER) for two fires in Siberia: fire F1 in October

2005 at taiga woodlands (53.5°N, 118.5–120.5°E) dominated by *Larix gmelinii* and *Betula fruticosa*, and fire F2 in August 2007 at taiga forest steppe (51.5°N, 109.5–112.0°E) dominated by *L. gmelinii*, *Larix sibirica* and *Pinus sylvestris* (Vasileva et al., 2017). MODIS indicated F1 and F2 were located in woody savanna and grassland, respectively. For the ratio of BC to CO, the ER for F1 and F2 were 6.1 and 6.3  $\mu\text{g}/\text{m}^3 \text{ ppm}^{-1}$ , respectively, according to Vasileva et al. (2017), while May et al. (2014) reported higher ERs of 16.7 and 21.8  $\mu\text{g}/\text{m}^3 \text{ ppm}^{-1}$  for Bamberg and Georgetown experiments. Therefore, using EF measured at Bamberg and Georgetown may not accurately represent the fires in northern Eurasia for developing FEI-NE.

## 2.2. Development of FEI-NE<sub>sp</sub>

For fire emission inventory development, bundling the plant species with the corresponding EF would be an ideal approach to lower the uncertainty. Although extensive literature reported the chamber experiments measured EF with fuel types records, the plant species information was unfortunately very limited for most places that were vulnerable to wildfires. In this study, we developed an emission inventory with species data and the corresponding EF over northern Eurasia. We used the plant species database in Eurasia from Schepaschenko et al. (2017), referred to as SchepaschenkoDB here and after. SchepaschenkoDB compiled the in situ sampling measurements from 159 publications over Eurasia and listed 57 dominant plant species in 9,613 locations for 48 ecoregions in Eurasia, the most comprehensive forest biomass structure data set for Eurasia to our knowledge (Schepaschenko et al., 2017). EF data were collected from the database reported by May et al. (2014), referred to as MayDB here-and-after, and the wildland fire emission factors database published by the United States Forest Service (<https://www.fs.usda.gov/rds/archive/Product/RDS-2014-0012/>), referred to as WFEFDB here-and-after. WFEFDB collected the emission factors for wildland fuels reported by 228 works of literature from the late 1960s through 2011 and 157 of them were supported with funding from the United States Forest Service. We used this database because it provided a detailed record of the dominant plant species of fuel type, and the records of plant species for a series of recently conducted experiments including chamber measurements and field campaigns. The categories of SchepaschenkoDB, MayDB, and WFEFDB were combined to rebuild the FEI-NE into FEI-NE<sub>sp</sub>.

Figure 2b described the flowchart of our mapping method to determine the EF to be used for individual fire. The fire locations from FEI-NE were first used to look up the plant species in SchepaschenkoDB. For each fire, to derive the corresponding EF of plant species (denoted as EF<sub>species</sub>), plant species in WFEFDB and MayDB were mapped to the same species in SchepaschenkoDB or fall into the same genus category. For example, EF for lodgepole pine from MayDB represented the EF for scots pine (*Pinus sylvestric*) indexed with species code 101\_Pi in SchepaschenkoDB. Since pine korean (105\_Pk), siberian pine (105\_Ps), dwarf pine (191\_Pd) and black pine (1011\_P and 1012\_P) were all species in the pinus genus, the EF represented their EFs for the pinus genus which was derived as the average for all pinus species recorded in WFEFDB and MayDB. Although scots pine and lodgepole pine were not the same pinus species, and there were also other pinus species (such as ponderosa pine) reported in WFEFDB and MayDB, we selected lodgepole pine as the representative species because it showed the most similar ER of BC/CO as that reported by Vasileva et al. (2017). May et al. (2014) reported the measured ER of BC/CO as 6.1  $\mu\text{g}/\text{m}^3 \text{ ppm}^{-1}$  for lodgepole pine with a moisture content of 45%, which was the closest value as compared with the ER measured in Siberia by Vasileva et al. (2017) as 6.1–6.3  $\mu\text{g}/\text{m}^3 \text{ ppm}^{-1}$  for wildfires with *B. fruticosa*, *L. gmelinii*, *L. sibirica*, and *P. sylvestris* as the dominant fuels. For the same reason and there was no EF reported for larch, lodgepole pine's EF was also selected to represent the larch's EF in northern Eurasia. We found EF for a total of 14 species in northern Eurasia. No fires were found with one of the species, Juniper, so 13 types of EF<sub>species</sub> were used in this study.

In case there was no detected plant species information or available EF<sub>species</sub> information for the dominant species from neither WFEFDB nor MayDB, the MODIS land cover would be used as the index to find the corresponding EF<sub>land cover</sub> for this fire. To derive the EF<sub>land cover</sub>, we first identified the top two dominant tree species for each land cover category in Eurasia. Then, we used the average of EFs for each species to calculate EF<sub>land cover</sub> (shown in Table S1 of the Supporting Information S1). For example, for the deciduous broadleaf forest, the primary tree species was 101\_Pi (*P. sylvestris*), and the secondary species was 110\_Oa (oak), so EFs for these two species were averaged to derive the EF<sub>land cover</sub> for the deciduous broadleaf forest. Once EF was determined, we applied it with the BA and FC from FEI-NE to build the species-dependent and land cover-dependent BC emission inventory as

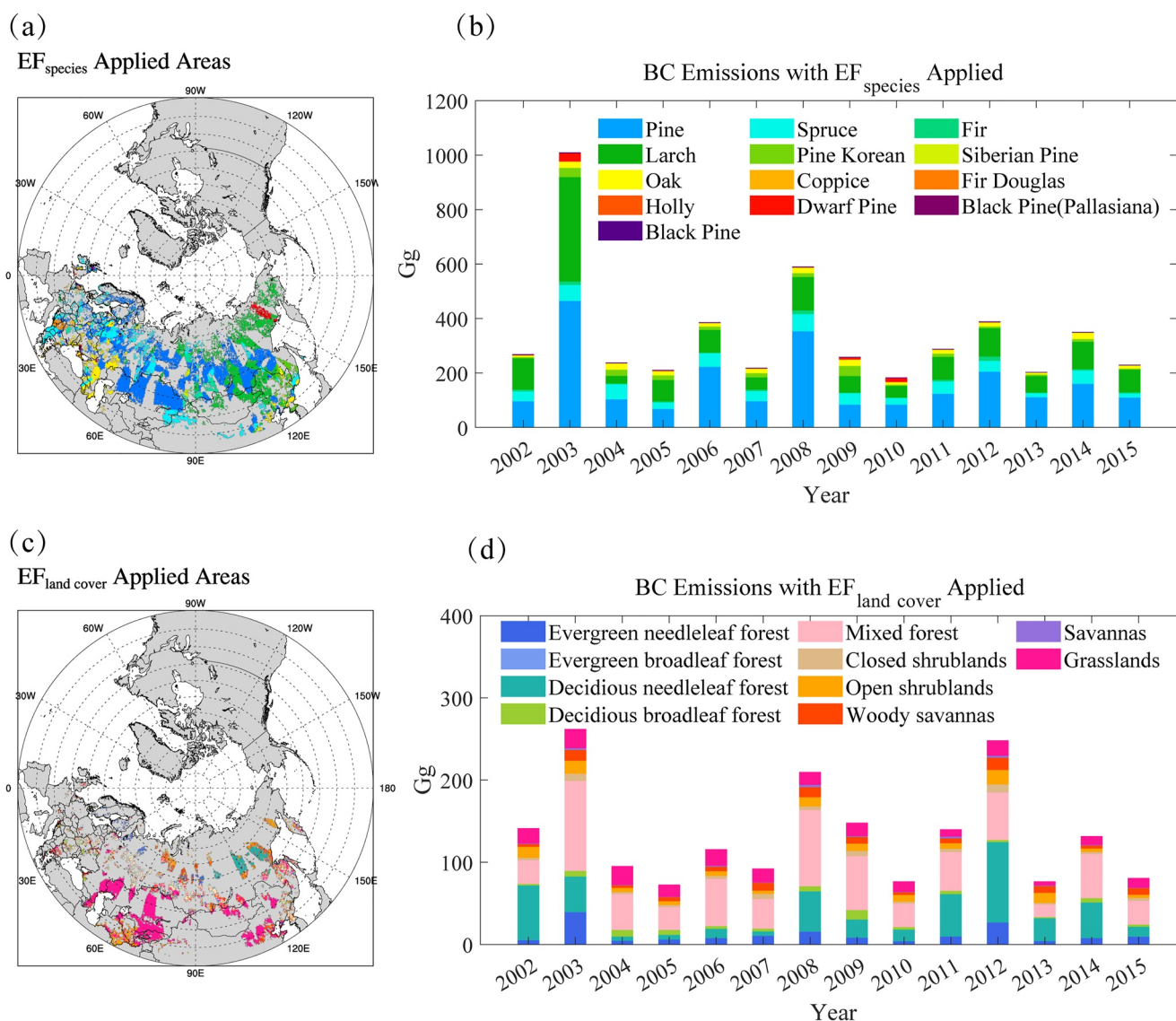


**Figure 3.** Areas applied with (a)  $EF_{species}$  and (c)  $EF_{land\ cover}$  BC emissions of (b) different plant species applied with  $EF_{species}$  and (d) different land cover types applied with  $EF_{land\ cover}$  over the period 2002–2015.

$FEI-NE_{sp}$ . The supplementary materials summarized the mapping details of  $EF_{species}$  and  $EF_{land\ cover}$  (see Tables S1 and S2 in Supporting Information S1).

### 2.3. Simulation Configurations

GEOS-Chem simulations with different sets of biomass-burning emission inputs were performed to probe into the model performance variation associated with emission factors. These scenarios include: (a). BASE: simulation with biomass burning BC emissions from GFEDv4.1s, (b). FEI-O: same as the BASE but with biomass burning emission in northern Eurasia replaced with FEI-NE, and (c). FEI-R: same as FEI-O but with biomass burning emission in northern Eurasia replaced with FEI-NE<sub>sp</sub>. For all these cases, anthropogenic BC emission was from the Community Emissions Data System (CEDS) inventory except using the Multi-resolution Emission Inventory

over China (MEI-C). All these scenarios were simulated for the years 2011 and 2012 with a full-year spin-off to provide the initial conditions in GEOS-Chem.

### 3. Results and Discussion

Figures 3a and 3c demonstrated the areas where  $EF_{\text{species}}$  and  $EF_{\text{land cover}}$  were applied respectively, while Figures 3b and 3d displayed the BC emissions calculated using these EFs from 2002 to 2015. In the northern Eurasia region, 69% of fires by area were applied with  $EF_{\text{species}}$  and 31% with  $EF_{\text{land cover}}$ . Pine, as the dominant fuel of wildfires, contributed the most abundant BC emissions at 34%, followed by larch at 21% and spruce at 8%. For fires where  $EF_{\text{land cover}}$  was applied, mixed forest contributed the most at 10%, followed by deciduous needle leaf forest at 7% and grassland at 3%. Compared to FEI-NE displayed in Figure 1i, the reconstructed FEI-NE<sub>sp</sub> is 33% lower due to the employment of different EFs.

Simulation results were compared with multiple observations to understand the impact of emission factors on the model performance. Figure 4a presented spatial distributions of biases between FEI-R and Ozone Monitoring Instrument (OMI) (Torres et al., 2007) and AEROSOL ROBOTIC NETWORK (AERONET) (Dubovik & King, 2000) observations during fire seasons (April–September). FEI-R generally underestimated AAOD in most parts of northern Eurasia compared to observations. Figure 4b showed the distribution of the root mean square error (RMSE) of AAOD between FEI-R and OMI observation. Lower latitude areas showed large values of RMSE but was most likely dominated by anthropogenic emission since northern Eurasia biomass burning was mainly over high latitude areas as shown in Figure 1. Figures 4c and 4d depicted the absolute differences in RMSE of AAOD between simulations. The main differences between FEI-O and the others were found in northeast Eurasia (A1, 90–150°E, 39–65°N) and northwest Eurasia (A2, 60–90°W, 50–63°N). Validation results with observations at AERONET stations were presented in Figures 4e and 4f. In Figure 4e, AERONET, OMI and MERRA-2 (Modern-Era Retrospective analysis for Research and Applications, version 2) reanalysis data (Gelaro et al., 2017) exhibited a peak of AAOD on 25 May 2011 at Yakutsk, in which FEI-O overestimated the AAOD significantly. Meanwhile, BASE could hardly capture this fire signal or temporal variations. At Tomsk in July 2012, all three cases underestimated the AAOD on most days. Since the dust AOD accounted for approximately 9% and 8% of the total AAOD on average respectively at Yakutsk in May 2011 and at Tomsk in July 2012, its presence in AERONET AAOD would not significantly affect the comparisons with the scenarios due to its small proportion (see Figure S1 in Supporting Information S1). As shown in Figure 4g, FEI-R exhibited the smallest normalized root mean square deviation (RMSD) among cases. Evaluation with OMI suggested the RMSD improved from 1.0 in FEI-O to 0.95 in FEI-R. Assessment with MERRA-2 showed that FEI-R gave the smallest RMSD and a relatively high correlation coefficient. When compared to AERONET, FEI-O had the largest RMSD of 1.13 while FEI-R had the smallest value of 1.06. These findings indicated that applying species and landcover-dependent EFs may better represent local fires in northern Eurasia. Dominant tree species in region A1, such as Scots pine (*P. sylvestris*) and larch, were considered “fire resisters,” with 42% and 41% of areas employing their respective EFs. Region A2 had pine and spruce as the dominant tree species accounting for approximately 98% of applied  $EF_{\text{species}}$ . The distinct differences in RMSE between simulations could be attributed to the relatively simple plant species diversity in Siberia (Osawa et al., 2010) in comparison to North America. The majority of fires in boreal North America occurred in mature stands of black spruce (*P. mariana*), jack pine (*Pinus banksiana*), and white spruce (*P. glauca*), which were known as “fire embracers” due to their high flammability and higher emission factors (Rogers et al., 2015; Rupp et al., 2002; Wirth, 2005). Subsequently, applying biome-based (BASE) or solely U.S. plant species-derived EFs (FEI-O) may not be able to accurately characterize the differences between boreal forests in northern Eurasia and those in North America. It is therefore vital to account for the regional and local variations in vegetation types when estimating emissions.

To assess model performance at higher altitudes, simulated BC concentrations were also evaluated using HIAPER (High-Performance Instrumented Airborne Platform for Environmental Research) Pole-to-Pole Observations (HIPPO) measurements (Wofsy, 2011) (Figure 4h). At the surface, the trends of FEI-R, FEI-O and the observa-

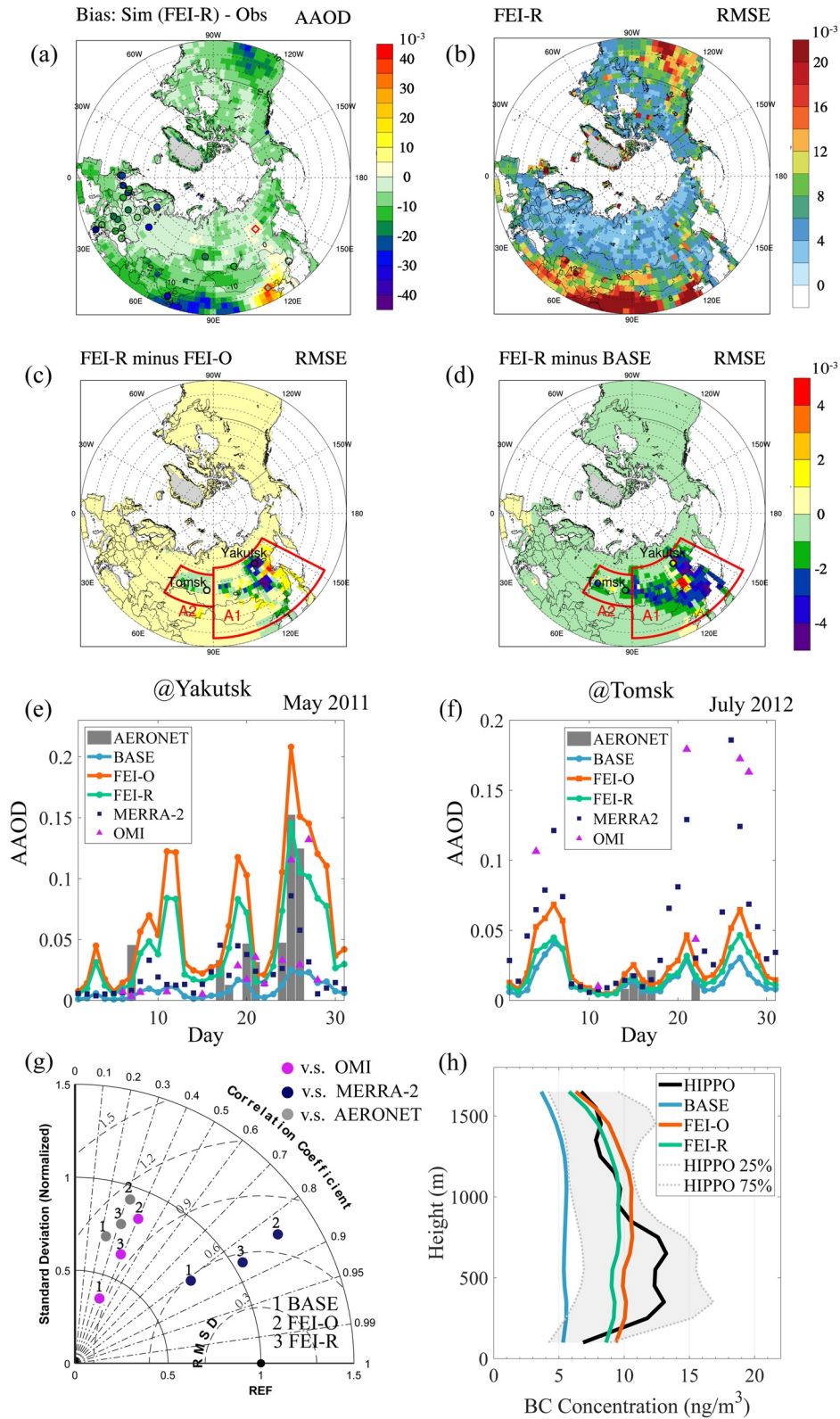


Figure 4.



tion were almost identical. FEI-R showed better agreement with observations in the vertical profile of the three cases from 900 to 1,600 m. The average BC concentration of BASE was smaller than 25% of the observation at 300–1,700 m, indicating that BASE may underestimate BC emissions at the surface. The averaged values of FEI-O and FEI-R were 25%–75% of observation below 1,700 m.

#### 4. Conclusions

Wildfires are rapidly expanding into boreal forests in response to emerging warmer and drier fire seasons (Zheng et al., 2023). Better characterizing biomass burning emissions, especially over high latitude areas, is of critical importance for improving the understanding of BC-related climate effects. Traditional biome-level emission factors may suffer from significant uncertainty. Motivated by the intercontinental differences in plant structure of North America and Eurasia, this study develops a species- and landcover-dependent wildfire black carbon emission inventory over northern Eurasia. Emission factors for a total of 14 species are compiled in northern Eurasia, with pine and larch being the dominant contributors to fires by area. The new inventory produces about 33% less black carbon emissions than current estimates based on FEI-NE and 61% more than those in GFED from 2002 to 2015. Simulation with species-specific emission factors improves the model performance mainly in northeast Eurasia with frequent fires, in terms of root mean square errors of AAOD at 550 nm compared to multiple observations. However, it shall be noted that the species-level emission factors may not always lead the simulation results closer to the actual conditions since the dominant species burned in each fire event may not necessarily be the most significant contributor to emissions. Uncertainties also remain in aerosol assumptions in the retrievals as well as model mechanisms. This study gives an implication for constraining the fire emissions uncertainty arising from the fuel types and improving the model performance.

This inventory can be expanded into a more comprehensive one containing multiple pollutants and covering a wider range of regions in future study. Since the plant species composition tends to be altered due to natural or human activities, updates of plant species information are necessary. Furthermore, it would be a challenging but necessary task for future research to characterize the vegetation types and EFs associated with combustion conditions. Incorporating the variability of combustion conditions and fuel types into emission estimates is critical for fire management applications and helps us enhance the accuracy of inventories.

**Figure 4.** (a) Spatial distribution of simulated aerosol absorbing optical depth (AAOD) at 550 nm bias against Ozone Monitoring Instrument (OMI) and AEROSOL ROBOTIC NETWORK (AERONET) from April to September for the year 2011 and 2012 under FEI-R scenario. AERONET stations are indicated with markers, and the bias against AERONET is overlaid on top of the bias against OMI. Red diamonds indicate the opposite sign of bias between AERONET and OMI, and black circles indicate the consistent sign of bias. (b) Root mean square error (RMSE, calculated in the form as  $RMSE = \sqrt{\frac{1}{N} \sum_{i=1}^n (Sim_i - Obs_i)^2}$ ) of AAOD between FEI-R and OMI observation during April–September 2011. Absolute differences in RMSE of AAOD (c) between FEI-R and FEI-O and (d) between FEI-R and BASE. Time series of daily simulated AAOD at 550 nm for the cases and AERONET site observations (e) at Yakutsk in May 2011 and (f) at Tomsk in July 2012. (g) Taylor diagram of evaluation statistics against OMI, AERONET and MERRA-2 (Modern-Era Retrospective analysis for Research and Applications, version2) for AAOD at 550 nm from April to September for year 2011 and 2012 in A1 and A2. Normalized root mean square deviation (RMSD) in the Taylor diagram is generated as  $RMSD = \sqrt{\frac{1}{N} \sum_{i=1}^n \left[ \left( Sim_i - \overline{Sim} \right) - \left( Obs_i - \overline{Obs} \right) \right]^2}$ . (h) Vertical profiles of observed and modeled BC concentrations in 68–75°N of July 2011 along HIPPO flight tracks.

## Data Availability Statement

Supporting Information S1 in this manuscript, including the compiled emission factors, is available at Figshare via <https://doi.org/10.6084/m9.figshare.22662178.v2>. The AERONET data are available at: [https://aeronet.gsfc.nasa.gov/new\\_web/data.html](https://aeronet.gsfc.nasa.gov/new_web/data.html); the OMI data can be reached here: <https://search.earthdata.nasa.gov/search?q=OMI/Aura>; the FEI-NE inventory can be downloaded via <https://www.fs.usda.gov/rds/archive/Product/RDS-2016-0036>; MODIS products can be found at <https://modis.gsfc.nasa.gov/data/>; the GFED data can be found at <https://www.globalfiredata.org/data.html>; the HIPPO data can be downloaded via [http://doi.org/10.3334/CDIAC/HIPPO\\_010](http://doi.org/10.3334/CDIAC/HIPPO_010); the MERRA-2 reanalysis data can be found at <https://gmao.gsfc.nasa.gov/reanalysis/MERRA-2/>.

## Acknowledgments

This work is supported by the National Natural Science Foundation of China (Grants 42075102, 91744208, 41925023, 41575073, and 41621005), the Ministry of Science and Technology of the People's Republic of China (Grant 2016YFC0200503) and the Frontiers Science Center for Critical Earth Material Cycling, Nanjing University (GeoX Grant 14380199). This research was also supported by the Collaborative Innovation Center of Climate Change, Jiangsu Province, and supported by the Frontiers Science Center for Critical Earth Material Cycling, Nanjing University (Grant 14380180). We greatly thank the High Performance Computing Center of Nanjing University for providing the computational resources used in this work.

## References

- Akagi, S. K., Yokelson, R. J., Wiedinmyer, C., Alvarado, M. J., Reid, J. S., Karl, T., et al. (2011). Emission factors for open and domestic biomass burning for use in atmospheric models. *Atmospheric Chemistry and Physics*, *11*(9), 4039–4072. <https://doi.org/10.5194/acp-11-4039-2011>
- Andreae, M. O. (2019). Emission of trace gases and aerosols from biomass burning—An updated assessment. *Atmospheric Chemistry and Physics*, *19*(13), 8523–8546. <https://doi.org/10.5194/acp-19-8523-2019>
- Andreae, M. O., & Merlet, P. (2001). Emission of trace gases and aerosols from biomass burning. *Global Biogeochemical Cycles*, *15*(4), 955–966. <https://doi.org/10.1029/2000GB001382>
- Bond, T. C., Doherty, S. J., Fahey, D. W., Forster, P. M., Berntsen, T., DeAngelo, B. J., et al. (2013). Bounding the role of black carbon in the climate system: A scientific assessment. *Journal of Geophysical Research: Atmospheres*, *118*(11), 5380–5552. <https://doi.org/10.1002/jgrd.50171>
- Bowman, D. M. J. S., Balch, J. K., Artaxo, P., Bond, W. J., Carlson, J. M., Cochrane, M. A., et al. (2009). Fire in the Earth system. *Science*, *324*(5926), 481–484. <https://doi.org/10.1126/science.1163886>
- Burling, I. R., Yokelson, R. J., Griffith, D. W. T., Johnson, T. J., Veres, P., Roberts, J. M., et al. (2010). Laboratory measurements of trace gas emissions from biomass burning of fuel types from the southeastern and southwestern United States. *Atmospheric Chemistry and Physics*, *10*(22), 11115–11130. <https://doi.org/10.5194/acp-10-11115-2010>
- Darmenov, A., & da Silva, A. (2015). The quick fire emissions dataset (QFED): Documentation of versions 2.1, 2.2, and 2.4. NASA Technical Report Series on Global Modeling and Data Assimilation, NASA TM-2015-104606 (Vol. 38). Retrieved from <https://gmao.gsfc.nasa.gov/pubs/docs/Darmenov796.pdf>
- Dong, X., Zhu, Q., Fu, J. S., Huang, K., Tan, J., & Tipton, M. (2019). Evaluating recent updated black carbon emissions and revisiting the direct radiative forcing in Arctic. *Geophysical Research Letters*, *46*(6), 3560–3570. <https://doi.org/10.1029/2018GL081242>
- Dubovik, O., & King, M. D. (2000). A flexible inversion algorithm for retrieval of aerosol optical properties from Sun and sky radiance measurements. *Journal of Geophysical Research*, *105*(D16), 20673–20696. <https://doi.org/10.1029/2000jd900282>
- Gelaro, R., McCarty, W., Suárez, M. J., Todling, R., Molod, A., Takacs, L., et al. (2017). The Modern-Era Retrospective analysis for Research and Applications, version 2 (MERRA-2). *Journal of Climate*, *30*(14), 5419–5454. <https://doi.org/10.1175/jcli-d-16-0758.1>
- Giglio, L., Randerson, J. T., & van der Werf, G. R. (2013). Analysis of daily, monthly, and annual burned area using the fourth-generation global fire emissions database (GFED4). *Journal of Geophysical Research: Biogeosciences*, *118*(1), 317–328. <https://doi.org/10.1002/jgrg.20042>
- Guenther, A. B., Jiang, X., Heald, C. L., Sakulyanontvittaya, T., Duhl, T., Emmons, L. K., & Wang, X. (2012). The model of emissions of gases and aerosols from nature version 2.1 (MEGAN2.1): An extended and updated framework for modeling biogenic emissions. *Geoscientific Model Development*, *5*(6), 1471–1492. <https://doi.org/10.5194/gmd-5-1471-2012>
- Hao, W. M., Petkov, A., Nordgren, B. L., Corley, R. E., Silverstein, R. P., Urbanski, S. P., et al. (2016). Daily black carbon emissions from fires in northern Eurasia for 2002–2015. *Geoscientific Model Development*, *9*(12), 4461–4474. <https://doi.org/10.5194/gmd-9-4461-2016>
- Haslett, S. L., Thomas, J. C., Morgan, W. T., Hadden, R., Liu, D., Allan, J. D., et al. (2018). Highly controlled, reproducible measurements of aerosol emissions from combustion of a common African biofuel source. *Atmospheric Chemistry and Physics*, *18*(1), 385–403. <https://doi.org/10.5194/acp-18-385-2018>
- Heringa, M. F., DeCarlo, P. F., Chirico, R., Tritscher, T., Dommen, J., Weingartner, E., et al. (2011). Investigations of primary and secondary particulate matter of different wood combustion appliances with a high-resolution time-of-flight aerosol mass spectrometer. *Atmospheric Chemistry and Physics*, *11*(12), 5945–5957. <https://doi.org/10.5194/acp-11-5945-2011>
- Huang, X., Song, Y., Zhao, C., Cai, X., Zhang, H., & Zhu, T. (2015). Direct radiative effect by multicomponent aerosol over China. *Journal of Climate*, *28*(9), 3472–3495. <https://doi.org/10.1175/JCLI-D-14-00365.1>
- Li, S., Liu, D., Hu, D., Kong, S., Wu, Y., Ding, S., et al. (2021). Evolution of organic aerosol from wood smoke influenced by burning phase and solar radiation. *Journal of Geophysical Research: Atmospheres*, *126*(8), e2021JD034534. <https://doi.org/10.1029/2021JD034534>
- Liu, T., Mickley, L. J., Marlier, M. E., DeFries, R. S., Khan, M. F., Latif, M. T., & Karambelas, A. (2020). Diagnosing spatial biases and uncertainties in global fire emissions inventories: Indonesia as regional case study. *Remote Sensing of Environment*, *237*, 111557. <https://doi.org/10.1016/j.rse.2019.111557>
- May, A. A., McMeeking, G. R., Lee, T., Taylor, J. W., Craven, J. S., Burling, I., et al. (2014). Aerosol emissions from prescribed fires in the United States: A synthesis of laboratory and aircraft measurements. *Journal of Geophysical Research: Atmospheres*, *119*(20), 11826–11849. <https://doi.org/10.1002/2014JD021848>
- Osawa, A., Zyryanova, O. A., Matsuura, Y., Kajimoto, T., & Wein, R. W. (2010). Permafrost ecosystems. *Ecological Studies*, *209*. <https://doi.org/10.1007/978-1-4020-9693-8>
- Popovich, O. B., Evangelou, N., Kobaev, V. O., Chichayeva, M. A., Eleftheriadis, K., Gregorić, A., & Kasimov, N. S. (2022). Siberian Arctic black carbon: Gas flaring and wildfire impact. *Atmospheric Chemistry and Physics*, *22*(9), 5983–6000. <https://doi.org/10.5194/acp-22-5983-2022>
- Prichard, S. J., Ottmar, R. D., & Anderson, G. K. (2006). *Consume 3.0 user's guide* (234 pp.). Pacific Northwest Research Station. Retrieved from [https://www.fs.usda.gov/pnw/fera/research/smoke/consume/consume30\\_users\\_guide.pdf](https://www.fs.usda.gov/pnw/fera/research/smoke/consume/consume30_users_guide.pdf)
- Ramanathan, V., & Carmichael, G. (2008). Global and regional climate changes due to black carbon. *Nature Geoscience*, *1*(4), 221–227. <https://doi.org/10.1038/ngeo156>

- Reid, J. S., Hyer, E. J., Prins, E. M., Westphal, D. L., Zhang, J., Wang, J., et al. (2009). Global monitoring and forecasting of biomass-burning smoke: Description of and lessons from the fire locating and modeling of burning emissions (FLAMBE) program. *IEEE Journal of Selected Topics in Applied Earth Observations and Remote Sensing*, 2(3), 144–162. <https://doi.org/10.1109/JSTARS.2009.2027443>
- Rogers, B. M., Soja, A. J., Goulden, M. L., & Randerson, J. T. (2015). Influence of tree species on continental differences in boreal fires and climate feedbacks. *Nature Geoscience*, 8(3), 228–234. <https://doi.org/10.1038/ngeo2352>
- Rupp, T. S., Starfield, A. M., Chapin, F. S., & Duffy, P. (2002). Modeling the impact of black spruce on the fire regime of Alaskan boreal forest. *Climatic Change*, 55(1/2), 213–233. <https://doi.org/10.1023/A:1020247405652>
- Schepaschenko, D., Shvidenko, A., Usoltsev, V., Lakyda, P., Luo, Y., Vasylyshyn, R., et al. (2017). A dataset of forest biomass structure for Eurasia. *Scientific Data*, 4(1), 170070. <https://doi.org/10.1038/sdata.2017.70>
- Sulla-Menashe, D., Gray, J. M., Abercrombie, S. P., & Friedl, M. A. (2019). Hierarchical mapping of annual global land cover 2001 to present: The MODIS Collection 6 Land Cover product. *Remote Sensing of Environment*, 222, 183–194. <https://doi.org/10.1016/j.rse.2018.12.013>
- Torres, O., Tanskanen, A., Veihelmann, B., Ahn, C., Braak, R., Bhartia, P. K., et al. (2007). Aerosols and surface UV products from Ozone Monitoring Instrument observations: An overview. *Journal of Geophysical Research*, 112(D24), D24S47. <https://doi.org/10.1029/2007jd008809>
- Urbanski, S. P., Hao, W. M., & Nordgren, B. (2011). The wildland fire emission inventory: Western United States emission estimates and an evaluation of uncertainty. *Atmospheric Chemistry and Physics*, 11(24), 12973–13000. <https://doi.org/10.5194/acp-11-12973-2011>
- van der Werf, G. R., Randerson, J. T., Giglio, L., Collatz, G. J., Mu, M., Kasibhatla, P. S., et al. (2010). Global fire emissions and the contribution of deforestation, savanna, forest, agricultural, and peat fires (1997–2009). *Atmospheric Chemistry and Physics*, 10(23), 11707–11735. <https://doi.org/10.5194/acp-10-11707-2010>
- van der Werf, G. R., Randerson, J. T., Giglio, L., van Leeuwen, T. T., Chen, Y., Rogers, B. M., et al. (2017). Global fire emissions estimates during 1997–2016. *Earth System Science Data*, 9(2), 697–720. <https://doi.org/10.5194/essd-9-697-2017>
- Vasileva, A., Moiseenko, K., Skorokhod, A., Belikov, I., Kopeikin, V., & Lavrova, O. (2017). Emission ratios of trace gases and particles for Siberian forest fires on the basis of mobile ground observations. *Atmospheric Chemistry and Physics*, 17(20), 12303–12325. <https://doi.org/10.5194/acp-17-12303-2017>
- Voulgarakis, A., & Field, R. D. (2015). Fire influences on atmospheric composition, air quality and climate. *Current Pollution Reports*, 1(2), 70–81. <https://doi.org/10.1007/s40726-015-0007-z>
- Wiedinmyer, C., Akagi, S. K., Yokelson, R. J., Emmons, L. K., Al-Saadi, J. A., Orlando, J. J., & Soja, A. J. (2011). The Fire INventory from NCAR (FINN): A high-resolution global model to estimate the emissions from open burning. *Geoscientific Model Development*, 4(3), 625–641. <https://doi.org/10.5194/gmd-4-625-2011>
- Wirth, C. (2005). Fire regime and tree diversity in boreal forests: Implications for the carbon cycle. *Forest Diversity and Function: Temperate and Boreal Systems*, 309–344. [https://doi.org/10.1007/3-540-26599-6\\_15](https://doi.org/10.1007/3-540-26599-6_15)
- Wofsy, S. C. (2011). HIPER Pole-to-Pole Observations (HIPPO): Fine-grained, global-scale measurements of climatically important atmospheric gases and aerosols. *Philosophical Transactions of the Royal Society A: Mathematical, Physical and Engineering Sciences*, 369(1943), 2073–2086. <https://doi.org/10.1098/rsta.2010.0313>
- Yokelson, R. J., Burling, I. R., Gilman, J. B., Warneke, C., Stockwell, C. E., de Gouw, J., et al. (2013). Coupling field and laboratory measurements to estimate the emission factors of identified and unidentified trace gases for prescribed fires. *Atmospheric Chemistry and Physics*, 13(1), 89–116. <https://doi.org/10.5194/acp-13-89-2013>
- Zheng, B., Chevallier, F., Ciais, P., Yin, Y., & Wang, Y. (2018). On the role of the flaming to smoldering transition in the seasonal cycle of African fire emissions. *Geophysical Research Letters*, 45(21), 11998–12007. <https://doi.org/10.1029/2018GL079092>
- Zheng, B., Ciais, P., Chevallier, F., Chuvieco, E., Chen, Y., & Yang, H. (2021). Increasing forest fire emissions despite the decline in global burned area. *Science Advances*, 7(39), eabh2646. <https://doi.org/10.1126/sciadv.abh2646>
- Zheng, B., Ciais, P., Chevallier, F., Yang, H., Canadell, J. G., Chen, Y., et al. (2023). Record-high CO<sub>2</sub> emissions from boreal fires in 2021. *Science*, 379(6635), 912–917. <https://doi.org/10.1126/science.ade0805>